3-1-2013

Mitochondrial Handling of Excess Ca^{2+} is Substrate-dependent with Implications for Reactive Oxygen Species Generation

Mohammed Aldakkak
Medical College of Wisconsin

David F. Stowe
Marquette University

Ranjan K. Dash
Medical College of Wisconsin

Amadou K.S. Camara
Medical College of Wisconsin

Mitochondrial Handling of Excess Ca^{2+} Is Substrate-Dependent with Implications for Reactive Oxygen Species Generation

Mohammed Aldakkak
Department of Anesthesiology, The Medical College of Wisconsin
Milwaukee, WI
David F. Stowe
Department of Anesthesiology, The Medical College of Wisconsin
Department of Physiology, The Medical College of Wisconsin
Cardiovascular Research Center, The Medical College of Wisconsin
Department of Anesthesiology, VA Medical Center Research Service
Department of Biomedical Engineering, Marquette University
Milwaukee, WI
Ranian K. Dash
Department of Physiology, The Medical College of Wisconsin
Biotechnology and Bioengineering Center, The Medical College of Wisconsin,
Milwaukee, WI
Amadou K.S. Camara
Department of Anesthesiology, The Medical College of Wisconsin
Cardiovascular Research Center, The Medical College of Wisconsin
Milwaukee, WI

Free Radical Biology and Medicine, Vol. 56 (March 2013): pg. 193-203. DOI.

Abstract

Aim: The mitochondrial electron transport chain is the major source of reactive oxygen species (ROS) during cardiac ischemia. Several mechanisms modulate ROS production; one is mitochondrial Ca^{2+} uptake. Here we sought to elucidate the effects of extra-mitochondrial Ca^{2+} (e[Ca^{2+}]) on ROS production (measured as H_2O_2 release) from complexes I and III.

Results: Mitochondria, isolated from guinea pig hearts, were pre-incubated with increasing concentrations of $CaCl_2$ and then energized with the complex I substrate Na^+-pyruvate or the complex II substrate Na^+-succinate. Mitochondrial H_2O_2 release rates were assessed after giving either rotenone or antimycin A to inhibit complex I or III, respectively. After pyruvate, mitochondria maintained a fully polarized membrane potential (Δψ, assessed using rhodamine 123) and were able to generate NADH (assessed using autofluorescence) even with excess e[Ca^{2+}] (assessed using CaGreen-5N), whereas they remained partially depolarized and did not generate NADH after succinate. This partial Δψ depolarization with succinate was accompanied by a large release of H_2O_2 (assessed using amplex red/horseradish peroxidase) with later addition of antimycin A. In the presence of excess e[Ca^{2+}], adding cyclosporine A to inhibit mitochondrial permeability transition pore (mPTP) opening restored Δψ and significantly decreased antimycin A-induced H_2O_2 release.

Conclusions: Succinate accumulates during ischemia to become the major substrate utilized by cardiac mitochondria. The inability of mitochondria to maintain a fully polarized Δψ under excess e[Ca^{2+}] when succinate, but not pyruvate, is the substrate may indicate a permeabilization of the mitochondrial membrane which enhances H_2O_2 emission from complex III during ischemia.

Keywords: complex III, mitochondrial permeability transition pore, succinate, Ca^{2+}

Introduction

Several key factors are involved in the injury sustained during cardiac ischemia and reperfusion (IR). Of these, production of reactive oxygen species (ROS) plays a very important role. Mitochondria are a major source of ROS in cardiomyocytes. In physiological states, ROS are formed during mitochondrial respiration but they are normally maintained at low levels by the endogenous matrix antioxidant

defenses [1, 2]. This small amount of ROS makes mitochondria very important for normal cellular function. In contrast, when ROS production exceeds the capacity of the scavenging system, as during ischemia, oxidative stress and concomitant damage occurs, leading to cell dysfunction and cell death.

Another key event in the injury sustained during IR is Ca^{2+}overload in the cytosol and organelles [3]. Even though Ca^{2+} is a crucial second messenger in modulating cellular function, extra-mitochondrial Ca^{2+} (e[Ca^{2+}]) overload is detrimental to mitochondrial function because it leads to opening of the mitochondrial permeability transition pore (mPTP), release of cytochrome *c* and other apoptotic factors, and apoptosis/necrosis [4, 5]. Excess e[Ca^{2+}] also induces injury by enhancing ROS emission and vice versa [6], although isolated mitochondrial studies have furnished discordant results for the concept of Ca^{2+}-induced ROS production. This variation likely stems from the different approaches and experimental conditions utilized. Nonetheless, a marked increase in ROS and excess accumulation of e[Ca^{2+}] and subsequently mitochondrial Ca^{2+} (m[Ca^{2+}]) during ischemia occur in parallel, as we have shown previously in isolated perfused hearts undergoing 30 min of global ischemia followed by reperfusion [7–10]. Interestingly, in these studies, we observed two phases of increased ROS (mainly superoxide anion, ($O_2^{\cdot -}$)), one upon initiating ischemia, and another during late ischemia (last 5 min). The latter phase was associated with irreversible IR injury because treatments that reduced IR injury caused less increase in ROS during the second phase with no effect during the first phase [7–9]. However, it is unknown if these two phases of increased ROS are derived from similar or different mitochondrial sources, and if excess e[Ca^{2+}]/m[Ca^{2+}] influences either or both of them.

$O_2^{\cdot -}$ is generated in the mitochondrion during cardiac ischemia from the electron transport chain (ETC) along the inner mitochondrial membrane (IMM) [11]. The ETC sustains progressive damage during ischemia as evidenced, in part, by a decrease in complex I activity during early ischemia [12, 13], and a decrease in complex III activity during late ischemia [13]. This causes electron leak and generation of $O_2^{\cdot -}$. The main sources of $O_2^{\cdot -}$ in highly metabolic cells are complexes I and III [14–17]. It remains uncertain which, if either, of these two complexes plays a major role in excess ROS production during

ischemia. Moreover, dynamic changes in the mitochondrial environment during ischemia (gradual increase in Ca^{2+}, change in available metabolites, impairment of ETC complexes) may shift $O_2^{\cdot -}$ generation between complexes I and III as ischemia progresses.

Therefore, in the present study we examined for changes in the dismutated product of $O_2^{\cdot -}$, H_2O_2, under conditions that may mimic the mitochondrial environment during early ischemia (low e[Ca^{2+}], impaired complex I, and pyruvate as the dominant substrate) or late ischemia (high e[Ca^{2+}], impaired complex III, and succinate as the dominant substrate [18, 19]). We observed a large increase in H_2O_2 release rate from complex III in succinate-supported mitochondria at a high e[Ca^{2+}], a condition that occurs during late ischemia. Furthermore, we monitored changes in mitochondrial bioenergetics that may modulate H_2O_2 release (O_2 consumption, membrane potential ($\Delta\psi$) and NADH) to help unravel the different potential mechanisms of ROS production under physiological (normal Ca^{2+}) and pathological (high Ca^{2+}) conditions.

Materials and Methods

All experiments were performed in accordance with the National Institutes of Health (NIH) Guide for the Care and Use of Laboratory Animals (NIH Publication No. 85–23, revised 1996) and were approved by the Institutional Animal Care and Use Committee of the Medical College of Wisconsin.

Mitochondrial isolation

Heart mitochondria were isolated from ketamine-anesthetized (50 mg/kg IP) guinea pigs (250–350 g) as described previously [20–22]. Briefly, ventricles were excised, placed in an isolation buffer (buffer A) that contained (in mM) 200 mannitol, 50 sucrose, 5 KH_2PO_4, 5 MOPS, 1 EGTA, and 0.1% BSA (all chemicals from Sigma, St. Louis, MO, USA), with pH adjusted to 7.15 with KOH. Ventricles were then minced into 1-mm^3 pieces. The suspension was homogenized in isolation buffer containing 5 U/ml protease (*Bacillus licheniformis*, Sigma, St. Louis, MO, USA), followed by differential centrifugation, and the final pellet was re-suspended in isolation buffer and kept on ice.

Free Radical Biology and Medicine, Vol. 56 (March 2013): pg. 193-203. DOI.

Protein content was determined by the Bradford method [23]. Mitochondrial suspension volume was adjusted to have 12.5 mg protein/ml. All isolation procedures were conducted at 4°C and all experiments were conducted at room temperature (25°C). For experiments, mitochondria were suspended in experimental buffer (buffer B) that contained (in mM) 130 KCl (EMD Chemicals, Gibbstown, NJ, USA), 5 K_2HPO_4, 20 MOPS, 0.001 $Na_4P_2O_7$ and 0.1% BSA (all chemicals from Sigma, St. Louis, MO, USA), pH 7.15 adjusted with KOH to a final concentration of 0.5 mg protein/ml. This insured that only 40 μM of EGTA was carried over from the isolation buffer (buffer A).

Mitochondrial O_2 consumption

O_2 consumption was measured polarographically using a respirometry system (System S 200A, Strathkelvin Instruments, Glasgow, Scotland). Respiration was initiated by adding 10 mM of the complex I substrate Na^+-pyruvate or the complex II substrate Na^+-succinate (Sigma, St. Louis, MO, USA). State 3 respiration was determined after adding 250 μM ADP (Sigma, St. Louis, MO, USA), and state 4 respiration was measured after complete phosphorylation of ADP to ATP. The respiratory control index (RCI) was calculated as the ratio of the rate of state 3 to state 4 respiration. Only mitochondria with an RCI of 10 or above with pyruvate or an RCI of 3 or above with succinate were used in the experiments. To assess effects of e[Ca^{2+}] on O_2 consumption, different [$CaCl_2$] (0, 50, 75, 100 μM) were added to the mitochondrial suspension before addition of substrates.

Experimental protocol for fluorescence measurements

Mitochondria were suspended in the respiration buffer (buffer B) which contained the appropriate fluorescent probe to assess levels of either H_2O_2, Δψ, or e[Ca^{2+}] while autofluorescence was used to monitor NADH. Increasing [$CaCl_2$] (0–100 μM) were added to the mitochondrial suspension (taking into account the amount of residual EGTA of 40 μM we estimate 100 μM $CaCl_2$ ≈ 120 nmole $CaCl_2$ /mg protein). This was followed by addition of 10 mM of either Na^+-pyruvate or Na^+-succinate. Then either the complex I blocker rotenone (10 μM; Sigma, St. Louis, MO, USA) or the complex III blocker

antimycin A (5 μM; Sigma, St. Louis, MO, USA) was added. In some experiments rotenone was added before adding succinate. Additional information on the protocols are given in the results section and the individual figures.

Mitochondrial fluorescence measurements

Mitochondria were suspended in buffer B in a 1 ml cuvette inside spectrophotometer (QM-8, Photon Technology International, Birmingham, NJ, USA). The rate of H_2O_2 release was measured using amplex red (12.5 μM, Molecular Probes, Eugene, OR, USA) in the presence of 0.1 U/ml horseradish peroxidase (Sigma, St. Louis, MO, USA) at excitation and emission wavelengths of 530 and 583 nm, respectively [21, 22]. H_2O_2 levels were calibrated over a range of 10–200 nM H_2O_2 (Sigma, St. Louis, MO, USA) added to buffer B in the absence of mitochondria and in the presence of amplex red and horseradish peroxidase. Changes in mitochondrial Δψ were monitored in the presence of the fluorescent dye rhodamine 123 (50 nM; Molecular Probes, Eugene, OR, USA) at excitation and emission wavelengths of 503 and 527 nm, respectively [21, 22]. Changes in e[Ca^{2+}] were monitored using the fluorescent probe CaGreen-5N hexapotassium salt (100 nM; Molecular Probes, Eugene, OR, USA) at excitation and emission wavelengths of 503 and 532 nm, respectively [24]. Mitochondrial NADH autofluorescence was monitored at an excitation wavelength of 350 and dual emission wavelengths of 460 nm and 405 nm. The ratio of 460/405 represents NADH [21].

Statistical analysis

Where appropriate, data are presented as mean ± SEM. Traces are representative for several experiments as indicated in figure legends. All data were compiled using Microsoft Excel and analyzed using one-way ANOVA and the Student-Newman-Keuls post hoc for multiple comparisons. The level for statistical significance was set to 5%, two tailed.

Results

Free Radical Biology and Medicine, Vol. 56 (March 2013): pg. 193-203. DOI.

H_2O_2 release rates were measured in isolated mitochondria with added $CaCl_2$ under two substrate conditions (Fig. 1). Complex I can produce $O_2^{\cdot -}$ by two mechanisms, the first of which is forward electron transfer (FET) when complex I is blocked (Fig. 1A). To test how added $CaCl_2$ affects H_2O_2 release, mitochondria were pre-incubated with 50, 75, or 100 μM $CaCl_2$ in the presence of 40 μM of EGTA carried over from the isolation buffer. Mitochondria were then energized with Na^+-pyruvate followed by rotenone (10 μM) to inhibit complex I. In the absence of added $CaCl_2$ (0 μM $CaCl_2$), rotenone increased H_2O_2 release to 0.46±0.05 pmole/mg/s. Addition of $CaCl_2$ caused a concentration-dependent increase in rotenone-induced H_2O_2 release rate; e.g. the presence of 100 μM $CaCl_2$ increased rotenone-induced H_2O_2 release by ~2 fold to 0.85±0.13 pmole/mg/s. The second mechanism of $O_2^{\cdot -}$ generation from complex I is reverse electron transfer (RET) from complex II to complex I with succinate as the sole substrate (Fig. 1B, between 100–200 s). Succinate without added $CaCl_2$ caused a much larger increase in H_2O_2 release rate (9.18±0.66 pmole/mg/s). Added $CaCl_2$ caused a concentration-dependent decrease in RET-induced H_2O_2 release to as low as 0.17±0.04 pmole/mg/s after adding 100 μM $CaCl_2$.

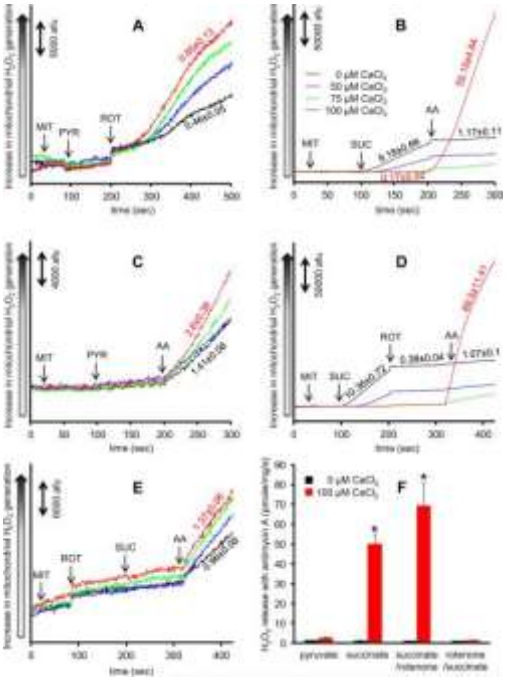

Fig. 1 Time dependent changes in H_2O_2 release rates in isolated mitochondria assessed using amplex red with horseradish peroxidase

Free Radical Biology and Medicine, Vol. 56 (March 2013): pg. 193-203. DOI.

Panel A shows H_2O_2 levels from inhibited complex I in pyruvate-energized mitochondria. Panel B shows H_2O_2 levels from complex I due to reversed electron transfer and from inhibited complex III in succinate-energized mitochondria. Panel C shows H_2O_2 levels from inhibited complex III in pyruvate-energized mitochondria. Panel D shows H_2O_2 levels from inhibited complex III in succinate-energized mitochondria but with rotenone added after succinate to prevent reverse electron transfer. Panel E shows H_2O_2 levels from inhibited complex III in succinate-energized mitochondria but with rotenone added before succinate to prevent reverse electron transfer. $CaCl_2$ was added before any other additions at time 0. Numbers indicate mean values ± (SEM) of pmole H_2O_2 emission/mg/s. The number of animals used ranged between 6–8 per group. Panel F shows a summary of the effects of added $CaCl_2$ on rates of H_2O_2 release under the four conditions (pyruvate, succinate, succinate first followed by rotenone, or rotenone first followed by succinate) with antimycin A. Columns represent mean values ± (SEM) of pmole H_2O_2 emission/mg/s. * indicates significant change in H_2O_2 release rate from inhibited complex III under high e[Ca^{2+}] in succinate or succinate/rotenone vs. pyruvate or rotenone/succinate-energized mitochondria. Abbreviations: MIT, mitochondria (0.5 mg/ml); PYR, pyruvate (10 mM); SUC, succinate (10 mM); ROT, rotenone (10 μM); AA, antimycin A (5 μM).

The other major source of $O_2^{\cdot -}$ generation is complex III. To study effects of Ca^{2+} on H_2O_2 release from complex III, mitochondria were pre-incubated with different [$CaCl_2$] and then energized with either pyruvate (Fig. 1C) or succinate (Fig. 1B); this was followed by antimycin A (5 μM) to block complex III. In pyruvate-energized mitochondria with no added $CaCl_2$, adding antimycin A enhanced H_2O_2 release to 1.41±0.08 pmole/mg/s. Addition of $CaCl_2$ caused a concentration-dependent increase in antimycin A-induced H_2O_2 release rate; e.g. the presence of 100 μM $CaCl_2$ increased antimycin A-induced H_2O_2 release by ~2 fold to 2.6±0.39 pmole/mg/s. In succinate-energized mitochondria and in the absence of $CaCl_2$, the high rate of H_2O_2 release (9.18±0.66 pmole/mg/s) due to RET decreased to 1.17±0.11 pmole/mg/s after adding antimycin A. However in the presence of 100 μM $CaCl_2$ the rate of antimycin A-induced H_2O_2 release increased markedly by ~40 fold (compared to antimycin A-induced H_2O_2 release in the absence of added $CaCl_2$) to 50.15±4.84 pmole/mg/s. With 75 μM $CaCl_2$, the rate of antimycin A-induced H_2O_2 release increased slightly compared to no added $CaCl_2$ and this was far less than that observed with addition of 100 μM $CaCl_2$.

These experiments (Fig. 1B) showed that elevated $CaCl_2$ markedly enhances H_2O_2 release from complex III in succinate-energized mitochondria. However, succinate induces RET and therefore in the next set of experiments we used a similar protocol as in Figure

1B but also added rotenone to inhibit RET. Succinate was given first followed by rotenone, and then by antimycin A (Fig. 1D). Even though rotenone almost completely blunted RET-induced H_2O_2 release (10.36±0.72 pmole/mg/s before rotenone, 0.38±0.04 pmole/mg/s after rotenone), antimycin A, in the presence of 100 μM $CaCl_2$, still caused a marked increase in H_2O_2 release (69.5±11.41 pmole/mg/s) compared to the slight increase in H_2O_2 release (1.07±0.1 pmole/mg/s) with no added $CaCl_2$. Interestingly, switching the order by adding rotenone before succinate (Fig. 1E) led to a different result, i.e., the marked increase in antimycin A-induced H_2O_2 release in the presence of 100 μM $CaCl_2$ was not observed (0.96±0.08 pmole/mg/s in the absence of $CaCl_2$, and 1.37±0.06 pmole/mg/s in the presence of added 100 μM $CaCl_2$).

A summary of the effects of added 100 μM $CaCl_2$ on rates of H_2O_2 release is shown under the four conditions (pyruvate, succinate, succinate followed by rotenone, rotenone followed by succinate) with inhibited complex III with antimycin A (Fig. 1F). The main observation from the above experiments is that Ca^{2+}-induced H_2O_2 release rate from complex III is substrate-dependent, i.e., excess e[Ca^{2+}] induced a larger increase in H_2O_2 release rate in succinate vs. pyruvate conditions, and this Ca^{2+}-induced effect was completely abolished when rotenone was added before adding succinate. Therefore, in the following experiments we focused only on these three conditions; i.e., effects of added $CaCl_2$ in pyruvate vs. succinate vs. rotenone followed by succinate-energized mitochondria with inhibited complex III (conditions that mimic those in Figures 1C, 1B, and 1E, respectively).

Because the results above showed differential effects of added $CaCl_2$ on H_2O_2 release from complex III based on the experimental conditions, we monitored m[Ca^{2+}] uptake by the disappearance of e[Ca^{2+}] into the matrix using CaGreen-5N. The same timeline protocol and conditions were used as in the H_2O_2 experiments. Adding pyruvate promoted m[Ca^{2+}] uptake (decrease of e[Ca^{2+}]) at each added [$CaCl_2$] (Fig. 2A). Adding antimycin A resulted in a small but significant concentration-dependent extrusion of Ca^{2+}. With succinate (Fig. 2B), m[Ca^{2+}] uptake was slower than that observed with pyruvate (Fig. 2A) with any added $CaCl_2$. In the presence of 100 μM $CaCl_2$, succinate-energized mitochondria took up less Ca^{2+} than did pyruvate-energized mitochondria (Fig. 2A vs. vs.2B).2B). Again, antimycin A resulted in

Ca^{2+} extrusion that was dependent on m[Ca^{2+}] uptake, except with added 100 μM $CaCl_2$ where m[Ca^{2+} uptake was already impaired with succinate as the substrate (Fig. 2B). In mitochondria first treated with rotenone (at time 0 s to prevent succinate-induced RET), m[Ca^{2+}] uptake after succinate was faster and greater (Fig. 2C) than that with succinate alone, and appeared in a pattern that was similar to that of pyruvate alone (Fig. 2A). Adding antimycin A after succinate caused a more pronounced concentration dependent Ca^{2+} extrusion compared to that after pyruvate (Fig. 2C vs. vs.2A2A).

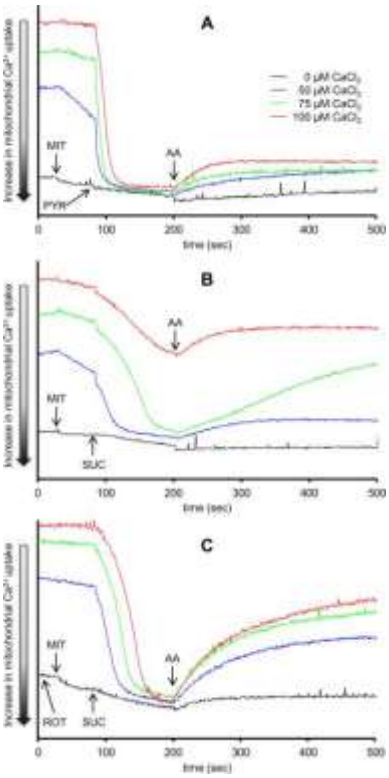

Fig. 2 Time dependent changes in extra-mitochondrial Ca^{2+} assessed using CaGreen-5N

Isolated mitochondria were energized with pyruvate (Panel A), succinate (Panel B), or succinate in the presence of rotenone (Panel C). Rotenone was added to the mitochondrial suspension at time 0. Mitochondria were pre-incubated with increasing [$CaCl_2$]. The number of animals used ranged between 6–8 per group. All figures have the same scale. Abbreviations: MIT, mitochondria (0.5 mg/ml); PYR, pyruvate (10 mM); SUC, succinate (10 mM); ROT, rotenone (10 μM); AA, antimycin A (5 μM).

Movement of Ca^{2+} into and out of the mitochondria is dependent on the Δψ and the Ca^{2+} gradient. Thus Δψ was also monitored using the same timeline protocol and conditions as above. Mitochondria

displayed a depolarized Δψ when pre-incubated with added $CaCl_2$. Addition of pyruvate led to complete Δψ repolarization regardless of the added $CaCl_2$ (Fig. 3A). In contrast, adding succinate to mitochondria pre-incubated with $CaCl_2$ led to a slower recovery of Δψ than after adding pyruvate, and at 100 μM $CaCl_2$ Δψ did not polarize (Fig. 3B). With rotenone added before succinate (to inhibit RET) a full Δψ polarization after adding succinate (Fig. 3C) occurred. The m[Ca^{2+}]-induced changes in Δψ with rotenone given before succinate were similar to those with pyruvate alone (Fig. 3A vs. vs.3C).3C). Adding antimycin A caused Δψ depolarization with all substrates regardless of the added $CaCl_2$, except in the presence of 100 μM $CaCl_2$ after succinate (Fig. 3B) because mitochondria were almost maximally depolarized.

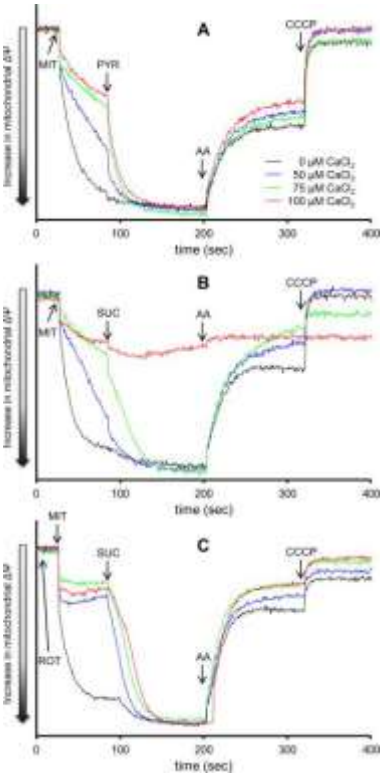

Fig. 3 Time dependent changes in mitochondrial inner membrane potential assessed using rhodamine 123

Isolated mitochondria were energized with pyruvate (Panel A), succinate (Panel B), or succinate in the presence of rotenone (Panel C). Rotenone was added to the mitochondrial suspension at time 0. Mitochondria were pre-incubated with increasing [$CaCl_2$]. The number of animals used ranged between 6–8 per group. All figures have the same scale. Abbreviations: MIT, mitochondria (0.5 mg/ml); PYR, pyruvate (10

Free Radical Biology and Medicine, Vol. 56 (March 2013): pg. 193-203. DOI.

mM); SUC, succinate (10 mM); ROT, rotenone (10 μM); AA, antimycin A (5 μM); CCCP, carbonyl cyanide-m-chlorophenylhydrazenone (4μM).

Because 100 μM $CaCl_2$ completely prevented Δψ polarization after succinate, we used a lower concentration of 80 μM $CaCl_2$, which allowed for a complete Δψ polarization with time after adding succinate (Fig. 4A). Antimycin A was then added before (at 200 s) or after (at 400 s) full Δψ polarization. Correspondingly, H_2O_2 release (Fig. 4B), measured under the same timeline protocol and conditions, was markedly increased when antimycin A was added at 200 s before Δψ became completely restored (Trace 1), whereas it was significantly reduced when antimycin A was added at 400 s when Δψ was completely repolarized (Trace 2).

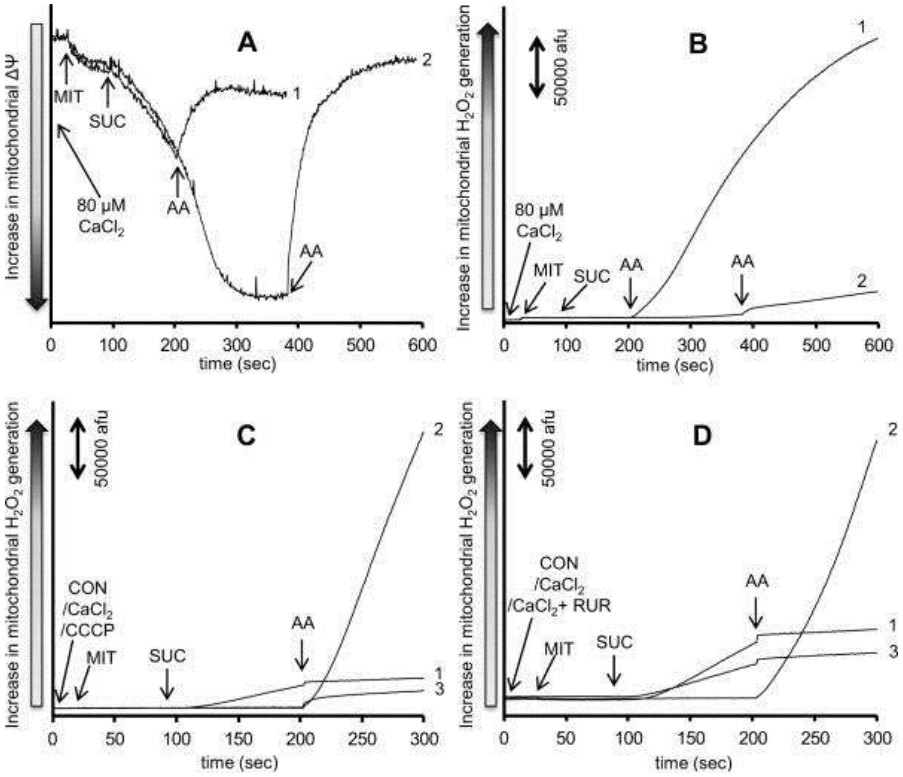

Fig. 4 Effect of membrane potential and extra-mitochondrial Ca^{2+} on H_2O_2 release due to complex III inhibition

Time dependent changes in mitochondrial inner membrane potential assessed using rhodamine 123 (Panel A) and H2O2 generation assessed using amplex red with horseradish peroxidase (Panel B) in succinate-energized mitochondria. Mitochondria were pre-incubated with 80 μM $CaCl_2$. Antimycin A was added at 200 s in Trace 1 and at 400 s in Trace 2. Panels C and D show time dependent changes in H_2O_2 levels in succinate-energized mitochondria. In Panel C, mitochondria were not pre-incubated

Free Radical Biology and Medicine, Vol. 56 (March 2013): pg. 193-203. DOI.

(Trace 1), pre-incubated with 100 μM $CaCl_2$ (Trace 2), or pre-incubated with 4 μM CCCP (Trace 3). In Panel D, mitochondria were not incubated (Trace 1), pre-incubated with 100 μM $CaCl_2$ (Trace 2), or pre-incubated with 100 μM $CaCl_2$ + 25 μM ruthenium red (Trace 3). The number of animals was 3 per group. Abbreviations: MIT, mitochondria (0.5 mg/ml); CON, control (H_2O); CCCP, carbonyl cyanide-m-chlorophenylhydrazenone (4μM); RUR, ruthenium red (25 μM); SUC, succinate (10 mM); AA, antimycin A (5 μM).

To test if the more rapid rate of H_2O_2 release at a partial Δψ depolarization is a result of the partially depolarized Δψ or the impediment in m[Ca^{2+}] uptake, we mimicked the conditions above by using either the uncoupler carbonyl cyanide-m-chlorophenylhydrazenone (CCCP, Sigma, St. Louis, MO, USA) (Fig. 4C) to depolarize Δψ (similar to depolarization observed with 100 μM $CaCl_2$), or the m[Ca^{2+}] uniporter inhibitor ruthenium red (Sigma, St. Louis, MO, USA) (Fig. 4D) to block m[Ca^{2+}] uptake. In mitochondria pre-incubated with 4 μM CCCP (Fig. 4C, Trace 3), adding antimycin A after succinate did not promote a large increase in H_2O_2 release as was observed when mitochondria were pre-incubated with 100 μM $CaCl_2$ (Fig. 4C, Trace 2). In mitochondria pre-incubated with 25 μM ruthenium red (Fig. 4D, Trace 3), adding antimycin A after succinate did not promote a large increase in H_2O_2 release as observed when mitochondria were pre-incubated only with 100 μM $CaCl_2$ (Fig. 4D, Trace 2).

The observed Δψ depolarization, impaired m[Ca^{2+}] uptake, and high rate of H_2O_2 generation after adding antimycin A in the presence of high [$CaCl_2$] and with succinate as the substrate may indicate a substantial role for mPTP opening. To test this, cyclosporine A (CsA, 0.5 μM, Sigma, St. Louis, MO, USA) was used to inhibit mPTP opening (Fig. 5). Adding CsA before succinate led to a full Δψ polarization (Fig. 5A), greater m[Ca^{2+}] uptake (Fig. 5B), and a significantly lower rate of H_2O_2 release after antimycin A (Fig. 5C).

Free Radical Biology and Medicine, Vol. 56 (March 2013): pg. 193-203. DOI.

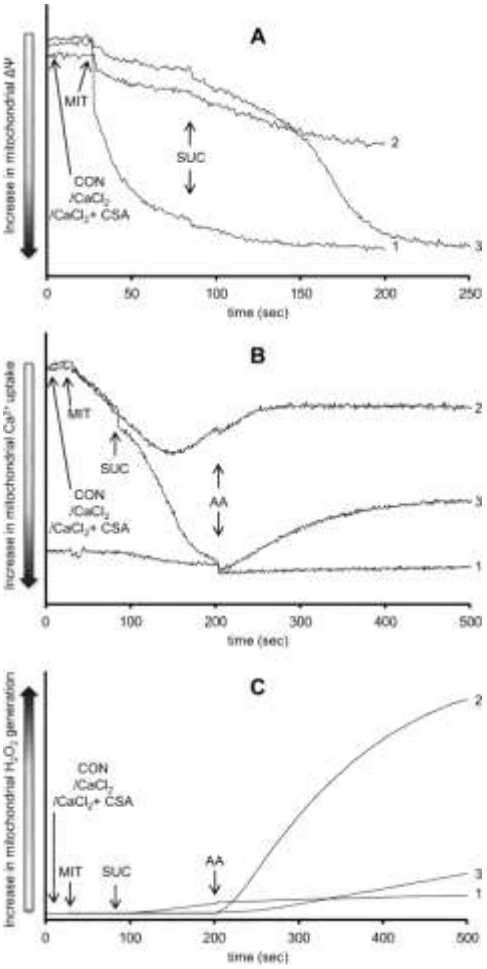

Fig. 5 Role of mitochondrial permeability transition pore in H_2O_2 release due to complex III inhibition

Time dependent changes in mitochondrial inner membrane potential (Panel A), extra-mitochondrial Ca^{2+} (Panel B), and H_2O_2 levels (Panel C) in succinate-energized mitochondria. In all panels, mitochondria were either not pre-incubated (Trace 1), pre-incubated with 100 μM $CaCl_2$ (Trace 2), or pre-incubated with 100 μM $CaCl_2$ + 0.5 μM cyclosporine A (Trace 3). The number of animals was 3 per group. Abbreviations: MIT, mitochondria (0.5 mg/ml); CON, control (H_2O); CSA, cyclosporine A (0.5 μM); SUC, succinate (10 mM); AA, antimycin A (5 μM).

The increase in H_2O_2 under succinate and elevated e[Ca^{2+}] conditions could be attributed to changes in the redox state (NADH). Therefore, NADH levels were monitored in mitochondria energized either with pyruvate (Fig. 6A), succinate (Fig. 6B), or rotenone given before succinate (Fig. 6C) at no added $CaCl_2$ (Trace 1) or in the presence of 100 μM $CaCl_2$ (Trace 2). Pyruvate led to an increase in NADH in the presence of 100 μM $CaCl_2$ similar to that observed with no

added $CaCl_2$ (Fig. 6A). Succinate, however, increased NADH only with 0 μM added $CaCl_2$ (Fig. 6B). Interestingly when rotenone was given before succinate, NADH gradually increased before even adding succinate with or without $CaCl_2$ (Fig. 6C). Later addition of succinate did not further increase NADH. In a modified protocol (Fig. 6D), mitochondria were pre-incubated with either 0 μM $CaCl_2$ (Trace 1) or 100 μM $CaCl_2$ (Trace 2) and then energized with succinate. Rotenone was then added followed by pyruvate in order to supply mitochondria with NADH without having a forward electron flow from complex I. Again, rotenone caused a gradual increase in NADH in mitochondria pre-incubated with 100 μM $CaCl_2$, and pyruvate caused an additional small increase in NADH. When the same protocol was used but with amplex red to measure H_2O_2, antimycin A still caused a large increase in H_2O_2 in mitochondria pre-incubated with 100 μM $CaCl_2$ (Fig. 6E).

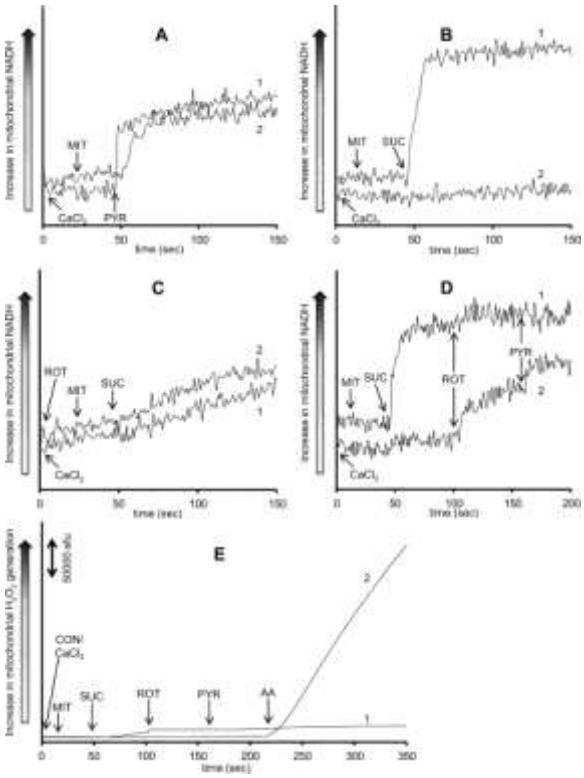

Fig. 6 Time dependent changes in NADH assessed using autofluorescence
Isolated mitochondria were energized with pyruvate (Panel A), succinate (Panel B), or succinate in the presence of rotenone (Panel C). Rotenone was added to the mitochondrial suspension at time 0. In a modified protocol, isolated mitochondria were energized with succinate, and then rotenone was added followed by pyruvate (Panel D). A similar protocol was used but with the addition of antimycin A after all other additions and in the presence of amplex red to measure H_2O_2 (Panel E). Mitochondria

Free Radical Biology and Medicine, Vol. 56 (March 2013): pg. 193-203. DOI.

were pre-incubated with either 0 μM $CaCl_2$ (Trace 1) or with 100 μM $CaCl_2$ (Trace 2). The number of animals ranged between 6–8 per group. All NADH figures have the same scale. Abbreviations: MIT, mitochondria (0.5 mg/ml); CON, control (H_2O); PYR, pyruvate (10 mM); SUC, succinate (10 mM); ROT, rotenone (10 μM); AA, antimycin A (5 μM).

Table 1 summarizes effects of added $CaCl_2$ on mitochondrial O_2 consumption during state 2 respiration (the state at which all experiments were conducted) and on RCI. State 2 respiration was monitored for 2 min before adding ADP to mimic the conditions in the above experiments (2 min between adding the substrate and adding antimycin A). Added $CaCl_2$ increased state 2 respiration with pyruvate and with rotenone plus succinate in a concentration-dependent manner. With succinate alone, $CaCl_2$ increased state 2 respiration in a concentration-dependent manner except with 100 μM added $CaCl_2$ in which state 2 respiration decreased in the first minute only and then increased in the second minute in a concentration-dependent manner. Table 1 also shows that $CaCl_2$ decreased RCI in a dose dependent manner under all substrate conditions even though mitochondria still exhibited well-coupled oxidative phosphorylation.

Table 1
Effects of increasing concentrations of $CaCl_2$ on mitochondrial O_2 consumption (μmole/h/mg) under various substrate conditions.

Substrate	[$CaCl_2$] (μM)	State 2 (min 1)	State 2 (min 2)	State 3	State 4	RCI
Pyruvate	0	0.7 ± 0.1	0.8 ± 0.1	14.1 ± 0.7	1 ± 0.1	14.6 ± 1.1
	50	0.9 ± 0*	1 ± 0*	15.2 ± 0.8	1.4 ± 0*	11 ± 0.6*
	75	0.9 ± 0*	1.2 ± 0*	15.2 ± 0.8	1.6 ± 0*	9.7 ± 0.4*
	100	1 ± 0*	1.3 ± 0*	14 ± 1.1	1.7 ± 0.1*	8.1 ± 0.5*
Succinate	0	3.4 ± 0.1	3.8 ± 0.2	19 ± 2	4 ± 0.2	4.7 ± 0.3
	50	3.5 ± 0.1	3.9 ± 0.2	18.1 ± 0.9	4 ± 0.1	4.5 ± 0.2
	75	3.7 ± 0.2	4.1 ± 0.2	17 ± 0.7	4.3 ± 0.2	4 ± 0.1
	100	2.3 ± 0.6	4.2 ± 0.3	13.3 ± 1.7	5.1 ± 0.3*	2.7 ± 0.4*
Rotenone/succinate	0	2.8 ± 0	3.2 ± 0	12.9 ± 0.2	3.7 ± 0.1	3.5 ± 0
	50	2.9 ± 0.2	3.4 ± 0.2	12.3 ± 0.8	3.7 ± 0.2	3.4 ± 0.1
	75	3.4 ± 0.1	3.9 ± 0.1	13.2 ± 0	4.1 ± 0.1	3.2 ± 0.1
	100	3.5 ± 0.1	4.1 ± 0.1	13 ± 0.1	4.4 ± 0.1	3 ± 0.1*

* $P < 0.05$, Ca^{2+} groups vs no Ca^{2+}.

Discussion

In this study we compared effects of Ca^{2+} on mitochondrial H_2O_2 emission from complexes I and III under different experimental conditions. These included utilizing substrates for complexes I and II, increasing e[Ca^{2+}], and the use of archetypical inhibitors of complexes I and III. We found a large rate of H_2O_2 emission due to complex III inhibition under conditions of elevated e[Ca^{2+}] and succinate as the only substrate, and that these conditions are conducive for mPTP opening as evidenced by Δψ depolarization, mitochondrial inability to

take up and retain Ca^{2+}, and the reversal of these effects with CsA. The novel finding is that prior, but not later, blockade of complex I with rotenone completely prevented mPTP opening and the subsequent increase in H_2O_2 release rate from inhibited complex III.

Complex III is the main source of ROS during late ischemia

Excess in m[Ca^{2+}] loading and ROS emission are often purported to be the two major factors causing cardiomyocytes death during IR injury [25]. In our previous studies of isolated perfused hearts undergoing 30 min of global ischemia [7–10], we observed a gradual accumulation of m[Ca^{2+}] throughout ischemia. On the other hand, ROS (mainly $O_2^{\cdot -}$) increased at two distinct time periods, an early phase within seconds upon initiating ischemia, and a late phase during the last 5 min of ischemia. The late phase was associated with an irreversible IR injury because treatments that reduced IR injury caused less increase in ROS during the second phase with no effect during the first phase. Therefore, we asked if these two phases of increasing ROS originate from the same/different sites of mitochondria, and if excess Ca^{2+} influences any or both of them.

First, despite the reduction in O_2 delivery during ischemia, there is still a considerable amount of O_2 present, therefore total anoxia is unlikely to exist even with clinically important ischemia [11]. Thus, cardiomyocytes can generate ROS during ischemia as we and others have shown [7–10, 26, 27]. Mitochondria are the main source of ROS generation in cardiomyocytes during ischemia [11]. Mitochondria generate $O_2^{\cdot -}$ from several sites [28] but the main sources in cardiomyocytes are complexes I and III of the ETC [1, 29]. Complex I generates $O_2^{\cdot -}$ by two modes [1, 28]; the first occurs when a high NADH/NAD^+ (FET) is accompanied by inhibition of complex I at the ubiquinone (Q) binding site [30–33]. The second mode occurs due to RET, a condition in which a highly reduced Q pool by succinate is associated with a high proton motive force [1, 33–36], which causes electrons to flow from complex II to complex I and to reduce NAD^+ to NADH [37]. RET supports high $O_2^{\cdot -}$ generation in the absence of ETC blockers [30, 38–42]. We propose that the early phase of ROS ($O_2^{\cdot -}$) increase that we observed in our previous isolated heart studies occurs

Free Radical Biology and Medicine, Vol. 56 (March 2013): pg. 193-203. DOI.

from complex I in the FET mode because: a) complex I activity decreases immediately upon initiating ischemia [13]; b) there is a sudden increase in NADH upon initiating ischemia that parallels the sudden increase in $O_2^{\cdot -}$ [7, 8, 43, 44]; c) this increase in ROS is not due to RET mode because succinate levels are not high during early ischemia [19]; and d) the increase in m[Ca^{2+}] during ischemia prevents RET likely due to the Ca^{2+}-induced decrease in Δψ [38, 45]. Indeed, $O_2^{\cdot -}$ generation by RET is highly dependent on Δψ such that a 10 mV decrease in Δψ eliminated $O_2^{\cdot -}$ generation by RET [46].

However, as ischemia progresses the ratio of NADH/NAD^+ decreases (less redox state) [8, 9] while succinate rises into the mM range [18, 19]. By late ischemia, m[Ca^{2+}] exceeds physiological levels. More importantly, complex III activity declines upon initiating ischemia and continues to decline gradually throughout late ischemia [13], which causes electrons to leak and generate $O_2^{\cdot -}$. Our current study shows that under conditions similar to those mentioned above and observed during late ischemia (high Ca^{2+}, high succinate, impaired complex III), we recorded the highest mitochondrial H_2O_2 release (Fig. 1B). Therefore, we propose that the large increase in H_2O_2 observed in our isolated mitochondrial study, which occurs due to complex III inhibition, represents the second phase of ROS production that we observed in our previous isolated perfused heart studies during late ischemia [7–10]. The large increase in H_2O_2 release observed in this study under the conditions noted above (high Ca^{2+}, high succinate, impaired complex III) cannot be attributed to RET because: a) the high e[Ca^{2+}] markedly reduced Δψ and as such prevented RET; and b) the large increase in H_2O_2 occurred even when rotenone was added after succinate to prevent RET (Fig. 1D). It could be argued that the [$CaCl_2$] used in our study are extremely high. However, mitochondria can sequester large amounts of Ca^{2+}, e.g. up to 400 nmole/mg protein [24], a much higher value than the maximum amount of $CaCl_2$ added in the present study, i.e. 120 nmole/mg protein, before collapse of Δψ. This was evident in our study as mitochondria were able to handle excess Ca^{2+} as shown by a reasonably high RCI with the substrate pyruvate. Indeed, it was reported that at a high range of Ca^{2+} load (up to 500 nmole/mg protein) mitochondria could maintain m[Ca^{2+}] between 1–5 μM [47]. This is likely ascribed to the rapid buffering via calcium-phosphate complex formation [48] or to other strong buffering components in the matrix. Moreover, we used 10 mM of Na^+-pyruvate

or Na^+-succinate which likely led to less m[Ca^{2+}] accumulation due to activation of mitochondrial Na^+/Ca^{2+} exchanger [49], which would extrude matrix Ca^{2+}.

Complex III generates H_2O_2 under depolarized Δψ

We have shown here that increasing e[Ca^{2+}] affects H_2O_2 release from complexes I and III. Unexpectedly, complex III inhibition caused a much larger H_2O_2 release in succinate than in pyruvate-energized mitochondria pre-incubated with high e[Ca^{2+}]. We hypothesized that this is attributed to differences in Δψ between these two conditions (pyruvate with high e[Ca^{2+}] vs. succinate with high e[Ca^{2+}]). Normally, a high proton motive force is associated with an increase in the probability of $O_2^{\cdot -}$ formation because semi-Q, which is capable of one electron reduction of O_2, becomes long lived when Δψ is sufficiently high [50]. Interestingly, this was not the case in our current study where high H_2O_2 release rates from complex III occurred under succinate with high e[Ca^{2+}], conditions in which was almost completely dissipated. This was further supported by the experiments in which we used a lower e[Ca^{2+}] (80 μM), chosen so that if the period before adding antimycin A was extended, then Δψ would recover completely (Fig. 4A) and mitochondria would sequester much of the added e[Ca^{2+}] (data not shown). Intriguingly, early addition of antimycin A, when Δψ was depolarized and e[Ca^{2+}] was elevated, led to a large increase in H_2O_2 release, but when addition of antimycin A was delayed until Δψ was fully polarized and much of the e[Ca^{2+}] was sequestered, H_2O_2 release was much reduced. These findings may initially indicate that inhibiting complex III in mitochondria with partially depolarized Δψ and/or elevated e[Ca^{2+}] leads to marked H_2O_2 release. However, adding the uncoupler CCCP to mimic high Ca^{2+}-induced Δψ depolarization did not cause a similar H_2O_2 release rate from inhibited complex III (Fig. 4C, Trace 3). Also, m[Ca^{2+}] uptake and not e[Ca^{2+}] appeared to instigate the large rate of H_2O_2 release from complex III in succinate-energized mitochondria, because preventing m[Ca^{2+}] uptake with ruthenium red significantly reduced H_2O_2 release from inhibited complex III (Fig. 4D, Trace 3). It is important to note that succinate-energized mitochondria were able to establish a fully polarized Δψ (Fig. 3B) when pre-incubated with 50 and 75 μM $CaCl_2$, and did not generate the large increase in H_2O_2

Free Radical Biology and Medicine, Vol. 56 (March 2013): pg. 193-203. DOI.

release observed with 100 μM $CaCl_2$. However, from the experiment in which 80 μM $CaCl_2$ was present, one can deduce that even at the lower concentrations of $CaCl_2$, early addition of antimycin A when Δψ is still depolarized may lead to a large increase in H_2O_2 release, i.e. if antimycin A was added between 100–120 s (Fig. 3B, Trace green).

High Ca^{2+} and succinate induce mitochondrial permeability

Although the above findings may seem paradoxical, i.e., significant H_2O_2 release from inhibited complex III in mitochondria with Ca^{2+}-and not CCCP-induced depolarized Δψ, these results may indicate a role for mPTP opening [51–53] in the loss of Δψ, subsequent accumulation of e[Ca^{2+}] with succinate, and a probable cause for the high H_2O_2 release rate from inhibited complex III. Indeed, this was confirmed by using CsA, an effective inhibitor of the mPTP in heart mitochondria [54], which restored Δψ (Fig. 5A), enabled succinate-energized mitochondria to take up and retain Ca^{2+} (Fig. 5B), and reduced antimycin A-induced H_2O_2 release (Fig. 5C). In fact, our findings agree with another study [55] which showed mPTP to mediate Ca^{2+}-induced ROS generation in brain mitochondria despite the inhibition of respiration, loss of Δψ and NADH. However, our present study shows that even before addition of antimycin A, Ca^{2+} induced mPTP opening only in succinate but not pyruvate-energized mitochondria. This is probably due to the lack of RET-induced NADH generation by complex I (Fig. 6B), which may lead to the loss of the NADH inhibitory effect on the mPTP reported earlier [56]. An alternative mechanism may involve the role of Δψ in mPTP opening as it was reported that increased Δψ depolarization is both necessary and sufficient to trigger mPTP opening [57]; however our experiments cannot resolve if Δψ depolarization precedes or if it is a consequence of mPTP opening. It is also possible that succinate impairs the m[Ca^{2+}] buffering capacity which leads to more available free Ca^{2+} that stimulates mPTP opening as was suggested in another study [58]. Nonetheless, caution must be taken when the results obtained in the current study (isolated mitochondria) are projected on the whole heart. While the conditions of high Ca^{2+} combined with high succinate such as during late ischemia may promote mPTP opening in isolated mitochondria, this may not be the case in the whole heart during late

Free Radical Biology and Medicine, Vol. 56 (March 2013): pg. 193-203. DOI.

ischemia due to cytosolic acidification which inhibits mPTP [51, 59, 60]. Nonetheless, it is worth mentioning that succinate and high Ca^{2+} together may lead to mitochondrial permeability that is different from mPTP. In fact, one study [52] indicated that under restricted substrate conditions (succinate only) and in the presence of Ca^{2+}, the IMM can be permeabilized. The authors suggested that this is a low-conductance permeability pathway that is different from the typical mPTP, and that this pathway is at least proton-permeable [52]. Our current study may support this notion by showing that inhibiting mPTP with CsA reduced but did not completely prevent the increase in H_2O_2 release from complex III induced by high Ca^{2+} (Fig. 5C). It is also possible that even the lower concentrations of $CaCl_2$ (50–75 μM) may lead to mPTP opening or some type of membrane permeability in succinate-energized mitochondria as evidenced by the slower recovery of Δψ in these groups (Fig. 3B). However, when given enough time, mitochondria were eventually able to take up all e[Ca^{2+}] (Fig. 2B) and to completely recover Δψ (Fig. 3B) which suggests a restored membrane permeability in these groups.

Mitochondrial permeability by succinate and high Ca^{2+} is required but not sufficient for H_2O_2 emission

It is important to note that while mPTP opening was sufficient to generate ROS as reported by Hansson et al. [55], this was not the case in our study in which mPTP opening did not induce any detectable H_2O_2, but was still required for the large release of H_2O_2 with subsequent inhibition of complex III by antimycin A. We attribute this to tissue differences (brain vs. heart) or because of a small H_2O_2 release that is not detectable using our technique. However, the large H_2O_2 release that occurs following inhibition of complex III could be explained in part by NADH loss. First, our study shows that succinate-energized mitochondria pre-incubated with high Ca^{2+} cannot generate NADH (Fig. 6B) due to the lack of RET. NAD(P)H is necessary to regenerate glutathione and thioredoxin [25], which together are the main H_2O_2 scavenging systems in mitochondria. Therefore, the large H_2O_2 release observed with complex III inhibition, which we proposed to happen by the end of ischemia, could simply result from less H_2O_2 scavenging rather than more H_2O_2 production. This agrees with the work of Aon et al. [61] who showed that under a more oxidized redox

potentials (such as during late ischemia), excess ROS occurs as a consequence of depletion of the ROS scavenger pool and not because of more ROS generation. However, oxidized redox potentials alone do not seem sufficient to explain the large H_2O_2 release from antimycin A-inhibited complex III that we observed in the current study. In a previous study we showed that CCCP oxidized NADH [21], but in the present study CCCP did not promote a substantial increase in H_2O_2 release from inhibited complex III (Fig. 4C, Trace 3) similar to that observed with elevated e[Ca^{2+}] (Fig. 4C, Trace 2). It remains possible that m[Ca^{2+}] loading may impair the scavenging system by a mechanism not related to NADH loss, i.e., Ca^{2+}-induced mitochondrial permeability may cause direct loss of glutathione [62], or alternatively Ca^{2+} may directly inhibit the activity of the scavenging enzymes [63].

Blocking complex I prevents excess H_2O_2 emission from inhibited complex III

Regardless of the mechanism for the permeabilization of mitochondrial membranes by succinate in the presence of high e[Ca^{2+}], all the injurious observations (impaired respiration, depolarization of Δψ, impaired m[Ca^{2+}] uptake, greater H_2O_2 emission) were abolished when rotenone was added before, but not after, adding succinate. It is probable that early inhibition of complex I with rotenone preserves the endogenous NADH as evidenced by the gradual increase in NADH after adding rotenone (Fig. 6C). This NADH is then used by the scavenging system to prevent the large increase in H_2O_2 release after adding antimycin A. However, this reasoning does not explain why adding rotenone after succinate did not prevent the large H_2O_2 release (Fig. 6E), although it still caused a similar gradual increase in NADH (Fig. 6D). An alternative mechanism may involve the role of rotenone as an mPTP blocker. Indeed, rotenone was shown to be even more effective than CsA as an mPTP blocker in U937 and KB cells [64]. This agrees with our findings showing that rotenone completely prevented Ca^{2+}-induced Δψ depolarization and the subsequent e[Ca^{2+}] accumulation in succinate-energized mitochondria. However if rotenone inhibits mPTP, it is not known if this is a direct effect or because it inhibits complex I which, interestingly, was suggested to be part of mPTP [65, 66]. Nonetheless, even though our present study gives limited clues as to the mechanism by which

rotenone prevents this large release of H_2O_2, it may highlight an important role for blocking complex I to reduce ROS production from complex III. In a previous study [8] we showed that reversible inhibition of complex I during ischemia decreased ROS and protected hearts against ischemic injury. We postulated that inhibiting complex I decreased electron transfer from complex I to complex III, thereby reduced electron leak, and $O_2^{\cdot -}$ generation at complex III during late ischemia [8]. Our current observations point toward an alternative mechanism for complex I blockade-mediated cytoprotection against ischemia.

Conclusion

Our previous isolated beating heart studies showed two phases of increase in ROS production during ischemia, an early one upon initiating ischemia and a late injurious phase during the last 5 min of 30 min global ischemia. The present study shows that under conditions that mimic the mitochondrial environment during late ischemia (high e[Ca^{2+}] with succinate as the main substrate) complex III becomes a major source of H_2O_2 release (Fig. 7). Moreover, early blockade of complex I can attenuate the rate of Ca^{2+}-induced H_2O_2 release from complex III.

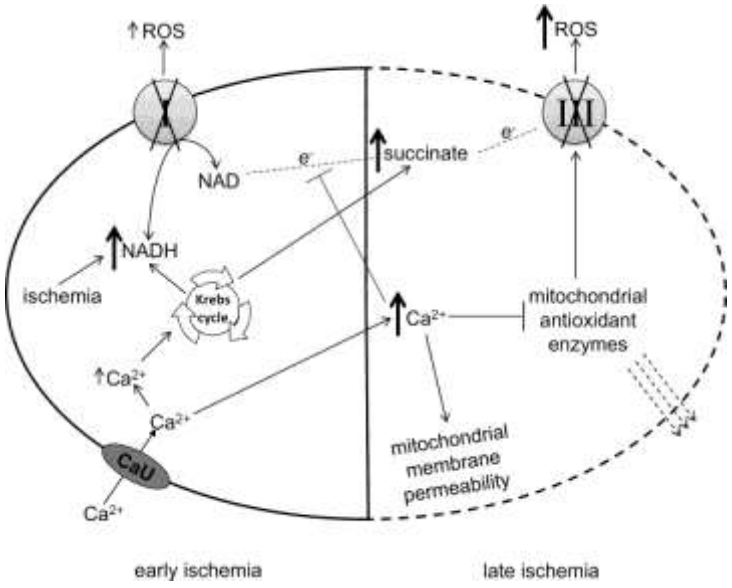

Fig. 7 Proposed role for complexes I and III in ROS generation as ischemia progresses

Early ischemia impairs electron flow through ETC and causes a sudden increase in

NADH [7–9], and a mild gradual increase in Ca2+ [7–9] and impairs complex I activity [13]. The increase in Ca2+ may increase NADH via the Krebs cycle and stimulate respiration (Table 1). More NADH leads to more electron flow through the impaired complex I and thus a mild increase in ROS [7–10]. Late ischemia causes a large increase in Ca2+ [7–9], accumulation of succinate [18, 19], and impaired complex III activity [13]. Excess Ca2+ causes mitochondrial membrane permeability [52, 67], Δψ depolarization which prevents reversed electron flow to complex I [38, 45] and the subsequent generation of NADH (Fig. 6B), and direct inhibition of the antioxidant systems [63]. Furthermore, the antioxidant enzymes may be lost due to increased membrane permeability [62]. This enhances ROS emission due to complex III impairment during late ischemia.

Highlights

- We measured mitochondrial H_2O_2 emission under different experimental conditions.
- Succinate and elevated Ca^{2+} caused mitochondrial membrane permeability.
- Succinate and elevated Ca^{2+} caused large increase in H_2O_2 from complex III.
- Early addition of rotenone prevented mitochondrial membrane permeability.
- Early addition of rotenone prevented the large increase in H_2O_2 from complex III.

Acknowledgment

This work was supported by grants from the National Institutes of Health (R01 HL095122, A.K.S. Camara / R.K. Dash; R01 HL089514, D.F. Stowe; P01 GM066730, Z.J. Bosnjak) and the Veterans Administration (VA Merit 8204-05P, D.F. Stowe)

Abbreviations

Δψ	membrane potential
AA	antimycin A (5 μM)
CCCP	carbonyl cyanide-m-chlorophenylhydrazenone (4 μM)
CON	control (H_2O)
CsA	cyclosporine A (0.5 μM)
ETC	electron transport chain

e[Ca^{2+}]	extra-mitochondrial Ca^{2+}
FET	forward electron transfer
IMM	inner mitochondrial membrane
IR	ischemia and reperfusion
m[Ca^{2+}]	mitochondrial Ca^{2+}
MIT	mitochondria (0.5 mg/ml)
mPTP	mitochondrial permeability transition pore
$O_2^{\cdot -}$	superoxide
PYR	pyruvate (10 mM)
Q	ubiquinone
RCI	respiratory control index
RET	reverse electron transfer
ROS	reactive oxygen species
ROT	rotenone (10 μM)
RUR	ruthenium red (25 μM)
SUC	succinate (10 mM)
TCA	tricarboxylic acid cycle

Footnotes

AUTHOR DISCLOUSRE STATEMENT No conflicts of interests

References

[1] Stowe DF, Camara AK. Mitochondrial reactive oxygen species production in excitable cells: modulators of mitochondrial and cell function. Antioxid Redox Signal. 2009;11:1373–1414.

[2] Tsutsui H, Kinugawa S, Matsushima S. Oxidative stress and mitochondrial DNA damage in heart failure. Circ J. 2008;72(Suppl A):A31–37.

[3] Stone D, Darley-Usmar V, Smith DR, O'Leary V. Hypoxia-reoxygenation induced increase in cellular Ca^{2+} in myocytes and perfused hearts: the role of mitochondria. J Mol Cell Cardiol. 1989;21:963–973.

[4] Crompton M. The mitochondrial permeability transition pore and its role in cell death. Biochem J. 1999;341(Pt 2):233–249.
[5] Halestrap AP, Clarke SJ, Javadov SA. Mitochondrial permeability transition pore opening during myocardial reperfusion--a target for cardioprotection. Cardiovasc Res. 2004;61:372–385.
[6] Peng TI, Jou MJ. Oxidative stress caused by mitochondrial calcium overload. Ann N Y Acad Sci. 2010;1201:183–188.
[7] Aldakkak M, Camara AK, Heisner JS, Yang M, Stowe DF. Ranolazine reduces Ca^{2+} overload and oxidative stress and improves mitochondrial integrity to protect against ischemia reperfusion injury in isolated hearts. Pharmacol Res. 2011;64:381–392.
[8] Aldakkak M, Stowe DF, Chen Q, Lesnefsky EJ, Camara AK. Inhibited mitochondrial respiration by amobarbital during cardiac ischaemia improves redox state and reduces matrix Ca^{2+} overload and ROS release. Cardiovasc Res. 2008;77:406–415.
[9] Aldakkak M, Stowe DF, Heisner JS, Spence M, Camara AK. Enhanced Na^+/H^+ exchange during ischemia and reperfusion impairs mitochondrial bioenergetics and myocardial function. J Cardiovasc Pharmacol. 2008;52:236–244.
[10] Kevin LG, Camara AK, Riess ML, Novalija E, Stowe DF. Ischemic preconditioning alters real-time measure of O_2 radicals in intact hearts with ischemia and reperfusion. Am J Physiol Heart Circ Physiol. 2003;284:H566–574.
[11] Becker LB. New concepts in reactive oxygen species and cardiovascular reperfusion physiology. Cardiovasc Res. 2004;61:461–470.
[12] Flameng W, Andres J, Ferdinande P, Mattheussen M, Van Belle H. Mitochondrial function in myocardial stunning. J Mol Cell Cardiol. 1991;23:1–11.
[13] Rouslin W. Mitochondrial complexes I, II, III, IV, and V in myocardial ischemia and autolysis. Am J Physiol. 1983;244:H743–748.
[14] Cadenas E, Davies KJ. Mitochondrial free radical generation, oxidative stress, and aging. Free Radic Biol Med. 2000;29:222–230.
[15] Chen Q, Camara AK, Stowe DF, Hoppel CL, Lesnefsky EJ. Modulation of electron transport protects cardiac mitochondria and decreases myocardial injury during ischemia and reperfusion. Am J Physiol Cell Physiol. 2007;292:C137–147.
[16] Chen Q, Vazquez EJ, Moghaddas S, Hoppel CL, Lesnefsky EJ. Production of reactive oxygen species by mitochondria: central role of complex III. J Biol Chem. 2003;278:36027–36031.
[17] Turrens JF, Boveris A. Generation of superoxide anion by the NADH dehydrogenase of bovine heart mitochondria. Biochem J. 1980;191:421–427.

[18] Kakinuma Y, Matsubara T, Hashimoto T, Sakamoto N. Myocardial metabolic markers of total ischemia in vitro. Nagoya J Med Sci. 1994;57:35–42.

[19] Starkov AA, Chinopoulos C, Fiskum G. Mitochondrial calcium and oxidative stress as mediators of ischemic brain injury. Cell Calcium. 2004;36:257–264.

[20] Aldakkak M, Stowe DF, Cheng Q, Kwok WM, Camara AK. Mitochondrial matrix K^+ flux independent of large-conductance Ca^{2+}-activated K^+ channel opening. Am J Physiol Cell Physiol. 2010;298:C530–541.

[21] Heinen A, Aldakkak M, Stowe DF, Rhodes SS, Riess ML, Varadarajan SG, Camara AK. Reverse electron flow-induced ROS production is attenuated by activation of mitochondrial Ca^{2+}-sensitive K^+ channels. Am J Physiol Heart Circ Physiol. 2007;293:H1400–1407.

[22] Heinen A, Camara AK, Aldakkak M, Rhodes SS, Riess ML, Stowe DF. Mitochondrial Ca^{2+}-induced K^+ influx increases respiration and enhances ROS production while maintaining membrane potential. Am J Physiol Cell Physiol. 2007;292:C148–156.

[23] Bradford MM. A rapid and sensitive method for the quantitation of microgram quantities of protein utilizing the principle of protein-dye binding. Anal Biochem. 1976;72:248–254.

[24] Wei AC, Liu T, Cortassa S, Winslow RL, O'Rourke B. Mitochondrial Ca^{2+} influx and efflux rates in guinea pig cardiac mitochondria: low and high affinity effects of cyclosporine A. Biochim Biophys Acta. 2011;1813:1373–1381.

[25] Camara AK, Lesnefsky EJ, Stowe DF. Potential therapeutic benefits of strategies directed to mitochondria. Antioxid Redox Signal. 2010;13:279–347.

[26] Becker LB, vanden Hoek TL, Shao ZH, Li CQ, Schumacker PT. Generation of superoxide in cardiomyocytes during ischemia before reperfusion. Am J Physiol. 1999;277:H2240–2246.

[27] Hess ML, Manson NH. Molecular oxygen: friend and foe. The role of the oxygen free radical system in the calcium paradox, the oxygen paradox and ischemia/reperfusion injury. J Mol Cell Cardiol. 1984;16:969–985.

[28] Murphy MP. How mitochondria produce reactive oxygen species. Biochem J. 2009;417:1–13.

[29] Brookes PS, Yoon Y, Robotham JL, Anders MW, Sheu SS. Calcium, ATP, and ROS: a mitochondrial love-hate triangle. Am J Physiol Cell Physiol. 2004;287:C817–833.

[30] Boveris A, Oshino N, Chance B. The cellular production of hydrogen peroxide. Biochem J. 1972;128:617–630.

[31] Kudin AP, Bimpong-Buta NY, Vielhaber S, Elger CE, Kunz WS. Characterization of superoxide-producing sites in isolated brain mitochondria. J Biol Chem. 2004;279:4127–4135.

[32] Kushnareva Y, Murphy AN, Andreyev A. Complex I-mediated reactive oxygen species generation: modulation by cytochrome c and NAD(P)$^+$ oxidation-reduction state. Biochem J. 2002;368:545–553.

[33] Kussmaul L, Hirst J. The mechanism of superoxide production by NADH:ubiquinone oxidoreductase (complex I) from bovine heart mitochondria. Proc Natl Acad Sci U S A. 2006;103:7607–7612.

[34] Adam-Vizi V, Chinopoulos C. Bioenergetics and the formation of mitochondrial reactive oxygen species. Trends Pharmacol Sci. 2006;27:639–645.

[35] Liu Y, Fiskum G, Schubert D. Generation of reactive oxygen species by the mitochondrial electron transport chain. J Neurochem. 2002;80:780–787.

[36] Votyakova TV, Reynolds IJ. DeltaPsi(m)-Dependent and -independent production of reactive oxygen species by rat brain mitochondria. J Neurochem. 2001;79:266–277.

[37] Chance B, Hollunger G. The interaction of energy and electron transfer reactions in mitochondria. I. General properties and nature of the products of succinate-linked reduction of pyridine nucleotide. J Biol Chem. 1961;236:1534–1543.

[38] Boveris A, Chance B. The mitochondrial generation of hydrogen peroxide. General properties and effect of hyperbaric oxygen. Biochem J. 1973;134:707–716.

[39] Croteau DL, ap Rhys CM, Hudson EK, Dianov GL, Hansford RG, Bohr VA. An oxidative damage-specific endonuclease from rat liver mitochondria. J Biol Chem. 1997;272:27338–27344.

[40] Korshunov SS, Korkina OV, Ruuge EK, Skulachev VP, Starkov AA. Fatty acids as natural uncouplers preventing generation of $O_2^{\cdot -}$ and H_2O_2 by mitochondria in the resting state. FEBS Lett. 1998;435:215–218.

[40] Kwong LK, Sohal RS. Substrate and site specificity of hydrogen peroxide generation in mouse mitochondria. Arch Biochem Biophys. 1998;350:118–126.

[42] Loschen G, Flohe L, Chance B. Respiratory chain linked H_2O_2 production in pigeon heart mitochondria. FEBS Lett. 1971;18:261–264.

[43] Camara AK, Aldakkak M, Heisner JS, Rhodes SS, Riess ML, An J, Heinen A, Stowe DF. ROS scavenging before 27°C ischemia protects hearts and reduces mitochondrial ROS, Ca^{2+} overload, and changes in redox state. Am J Physiol Cell Physiol. 2007;292:C2021–2031.

[44] Stowe DF, Aldakkak M, Camara AK, Riess ML, Heinen A, Varadarajan SG, Jiang MT. Cardiac mitochondrial preconditioning by Big Ca^{2+}-sensitive

K^+ channel opening requires superoxide radical generation. Am J Physiol Heart Circ Physiol. 2006;290:H434–440.

[45] Hansford RG, Hogue BA, Mildaziene V. Dependence of H_2O_2 formation by rat heart mitochondria on substrate availability and donor age. J Bioenerg Biomembr. 1997;29:89–95.

[46] Tretter L, Mayer-Takacs D, Adam-Vizi V. The effect of bovine serum albumin on the membrane potential and reactive oxygen species generation in succinate-supported isolated brain mitochondria. Neurochem Int. 2007;50:139–147.

[47] Chalmers S, Nicholls DG. The relationship between free and total calcium concentrations in the matrix of liver and brain mitochondria. J Biol Chem. 2003;278:19062–19070.

[48] Wei AC, Liu T, Winslow RL, O'Rourke B. Dynamics of matrix-free Ca^{2+} in cardiac mitochondria: two components of Ca^{2+} uptake and role of phosphate buffering. J Gen Physiol. 2012;139:465–478.

[49] Agarwal B, Camara AK, Stowe DF, Bosnjak ZJ, Dash RK. Enhanced charge-independent mitochondrial free Ca^{2+} and attenuated ADP-induced NADH oxidation by isoflurane: Implications for cardioprotection. Biochim Biophys Acta. 2012;1817:453–465.

[50] Korshunov SS, Skulachev VP, Starkov AA. High protonic potential actuates a mechanism of production of reactive oxygen species in mitochondria. FEBS Lett. 1997;416:15–18.

[51] Bernardi P, Vassanelli S, Veronese P, Colonna R, Szabo I, Zoratti M. Modulation of the mitochondrial permeability transition pore. Effect of protons and divalent cations. J Biol Chem. 1992;267:2934–2939.

[52] Brustovetsky N, Dubinsky JM. Dual responses of CNS mitochondria to elevated calcium. J Neurosci. 2000;20:103–113.

[53] Novgorodov SA, Gudz TI, Milgrom YM, Brierley GP. The permeability transition in heart mitochondria is regulated synergistically by ADP and cyclosporin A. J Biol Chem. 1992;267:16274–16282.

[54] Novgorodov SA, Gudz TI, Brierley GP, Pfeiffer DR. Magnesium ion modulates the sensitivity of the mitochondrial permeability transition pore to cyclosporin A and ADP. Arch Biochem Biophys. 1994;311:219–228.

[55] Hansson MJ, Mansson R, Morota S, Uchino H, Kallur T, Sumi T, Ishii N, Shimazu M, Keep MF, Jegorov A, Elmer E. Calcium-induced generation of reactive oxygen species in brain mitochondria is mediated by permeability transition. Free Radic Biol Med. 2008;45:284–294.

[56] Haworth RA, Hunter DR. Allosteric inhibition of the Ca^{2+}-activated hydrophilic channel of the mitochondrial inner membrane by nucleotides. J Membr Biol. 1980;54:231–236.

[57] Petronilli V, Cola C, Bernardi P. Modulation of the mitochondrial cyclosporin A-sensitive permeability transition pore. II. The minimal

requirements for pore induction underscore a key role for transmembrane electrical potential, matrix pH, and matrix Ca^{2+} J Biol Chem. 1993;268:1011–1016.

[58] Gogvadze V, Norberg E, Orrenius S, Zhivotovsky B. Involvement of Ca^{2+} and ROS in alpha-tocopheryl succinate-induced mitochondrial permeabilization. Int J Cancer. 2010;127:1823–1832.

[59] Halestrap AP. Calcium-dependent opening of a non-specific pore in the mitochondrial inner membrane is inhibited at pH values below 7. Implications for the protective effect of low pH against chemical and hypoxic cell damage. Biochem J. 1991;278(Pt 3):715–719.

[60] Haworth RA, Hunter DR. The Ca^{2+}-induced membrane transition in mitochondria. II. Nature of the Ca^{2+} trigger site. Arch Biochem Biophys. 1979;195:460–467.

[61] Aon MA, Cortassa S, O'Rourke B. Redox-optimized ROS balance: a unifying hypothesis. Biochim Biophys Acta. 2010;1797:865–877.

[62] Votyakova TV, Reynolds IJ. Ca^{2+}-induced permeabilization promotes free radical release from rat brain mitochondria with partially inhibited complex I. J Neurochem. 2005;93:526–537.

[63] Zoccarato F, Cavallini L, Alexandre A. Respiration-dependent removal of exogenous H_2O_2 in brain mitochondria: inhibition by Ca^{2+} J Biol Chem. 2004;279:4166–4174.

[64] Chauvin C, De Oliveira F, Ronot X, Mousseau M, Leverve X, Fontaine E. Rotenone inhibits the mitochondrial permeability transition-induced cell death in U937 and KB cells. J Biol Chem. 2001;276:41394–41398.

[65] Fontaine E, Bernardi P. Progress on the mitochondrial permeability transition pore: regulation by complex I and ubiquinone analogs. J Bioenerg Biomembr. 1999;31:335–345.

[66] Fontaine E, Eriksson O, Ichas F, Bernardi P. Regulation of the permeability transition pore in skeletal muscle mitochondria. Modulation By electron flow through the respiratory chain complex i. J Biol Chem. 1998;273:12662–12668.

[67] Baines CP. The mitochondrial permeability transition pore and ischemia-reperfusion injury. Basic Res Cardiol. 2009;104:181–188.

About the Authors

Corresponding author: Amadou K.S. Camara Ph.D., M4280, The Medical College of Wisconsin, 8701 Watertown Plank Road, Milwaukee, WI 53226, USA. Tel: 001-414-456-5624, Fax: 001-414-456-6507, Email: aksc@mcw.edu

Mohammed Aldakkak, maldakka@mcw.edu

Free Radical Biology and Medicine, Vol. 56 (March 2013): pg. 193-203. DOI.

David F Stowe, dfstowe@mcw.edu

Ranjan K Dash, rdash@mcw.edu